UCRL-53470
Distribution Category UC-70

Petrologic and Geochemical Characterization of the Bullfrog Member of the Crater Flat Tuff: Outcrop Samples Used in Waste Package Experiments

K. G. Knauss

Manuscript date: September 1983

LAWRENCE LIVERMORE NATIONAL LABORATORY
University of California • Livermore, California • 94550

Available from: National Technical Information Service • U.S. Department of Commerce
5285 Port Royal Road • Springfield, VA 22161 • $7.00 per copy • (Microfiche $4.50)

Contents

Petrologic and Geochemical Characterization of the Bullfrog Member of the Crater Flat Tuff: Outcrop Samples Used in Waste Package Experiments

Abstract

In support of the Waste Package Task within the Nevada Nuclear Waste Storage Investigation (NNWSI), experiments on hydrothermal rock/water interaction, corrosion, thermomechanics, and geochemical modeling calculations are being conducted. All of these activities require characterization of the initial bulk composition, mineralogy, and individual phase geochemistry of the potential repository host rock. This report summarizes the characterization done on samples of the Bullfrog Member of the Crater Flat Tuff (Tcfb) used for Waste Package experimental programs.

Introduction

Until late 1982 one of the four stratigraphic units considered potentially favorable for siting a repository in tuff was cooling unit II of the Bullfrog Member of the Crater Flat Tuff (Tcfb) (Bish et al., 1981). Early Waste Package experimental work used Tcfb; thus, it was necessary to acquire large quantities of material suitable for the testing program. Since material from core taken from Yucca Mountain was not available in sufficient quantity to supply this need, outcrop samples of Tcfb were selected to provide material for this purpose.

To understand the hydrothermal interaction between rock and water in the waste package environment, the mineralogic and geochemical character of the tuff must be well known. A variety of techniques was employed to characterize this material: transmitted and reflected light optical microscopy, x-ray diffraction (XRD) analyses, neutron activation analyses (NAA), gas adsorption surface area analyses (BET), scanning electron microscopy (SEM), and electron microprobe analyses (EMP) using both semiquantitative energy dispersive spectrometry (EDS) and quantitative wavelength dispersive spectrometry (WDS).

This report summarizes the results of this characterization of Tcfb material used in all Waste Package experiments in the various subtasks that required tuff to be present for conditioning water (e.g., studies on canister corrosion, backfill, and waste form) or a knowledge of the geochemical nature of the tuff for modeling (e.g., geochemical or thermal modeling).

Source of Material

Based on a correlation of corelogs, geophysical logs, mineralogy, and physical properties of core from holes G-1, G-2, UE25a-1, and UE25b-1, the proposed repository horizon within the Tcfb was defined as an interval ~340 to 2545 ft referenced to hole G-1. The petrologic and geochemical characteristics of this interval in several locations throughout the repository block are described in previous reports (Heiken and Bevier, 1979; Sykes et al., 1979; Bish et al., 1981; Caporuscio et al., 1982; Broxton et al., 1982; Scott and Castellanos, 1982).

New data from exploratory drilling, mapping, and petrographic studies in the Bare Mountain-Crater Flat area (Orkild, 1983; Carr, 1982) have suggested the source of the Crater Flat Tuffs to be two calderas in the Crater Flat area (not the Sleeping Butte caldera, as previously believed, Byers et al., 1976). The Tram Member was erupted from the northernmost of these calderas, while the Bullfrog and overlying Prow Pass Members were erupted from the southernmost caldera. Although poorly exposed partial sections of Tcfb are shown in areas with existing map coverage, the outcrops

were not suitable for precise location within the section. However, approximately 8-1/2 miles NW of Lathrop Wells (Nevada Coordinates N705,400' and E538,800') an excellent section of Tcfb is exposed along an arroyo on the southwest spur of Yucca Mountain.

This outcrop is located on the presently unmapped Big Dune 15' topographic map and was first shown to me by Bruce Crowe, Los Alamos National Laboratory, Los Alamos, NM (LANL). At this location the Tcfb section overlies a bedded, reworked tuff possibly containing fragments of the Grouse Canyon Member of the Belted Range Tuff (Fig. 1). Moving up this section, the Tcfb rapidly progresses from a nonwelded base into a moderately developed vitrophyre (Fig. 2). The presence of a vitrophyre suggests that the emplacement temperature was considerably higher than beneath Yucca Mountain near the repository block where no vitrophyre is observed. Also, at this location the unit is several hundred feet thick. The unit progresses to a thick zone of moderately welded, devitrified, slightly vapor phase altered core (Fig. 3). The top of the unit is nonwelded, pumiceous, and intensely vapor-phase altered. The Tcfb is overlain by a breccia consisting of Tcfb related material indicating relative proximity to the Bullfrog caldera; the breccia owes its origin to caldera collapse (Fig. 4).

At the site selected for sampling (Fig. 5), large blocks of material were removed, labeled, and shipped to Lawrence Livermore National Laboratory, Livermore, CA (LLNL) for further pretreatment. In some cases, the large blocks were sent directly to other investigators with no pretreatment. This was true for David G. Coles, Pacific Northwest Laboratories, Richland, WA, and James D. Byerlee, U.S. Geological Survey, Menlo Park, CA (USGS).

Sample Preparation

For all work done at LLNL, the large blocks of Tcfb were first trimmed with a large rock saw to remove weathered material (if any) along joints

Figure 1. Base of Bullfrog Member overlying a bedded, reworked tuff.

Figure 2. View up the section from below the vitrophyre within the Bullfrog Member. Darker material forming the ledge in the center of the photo is the vitrophyre.

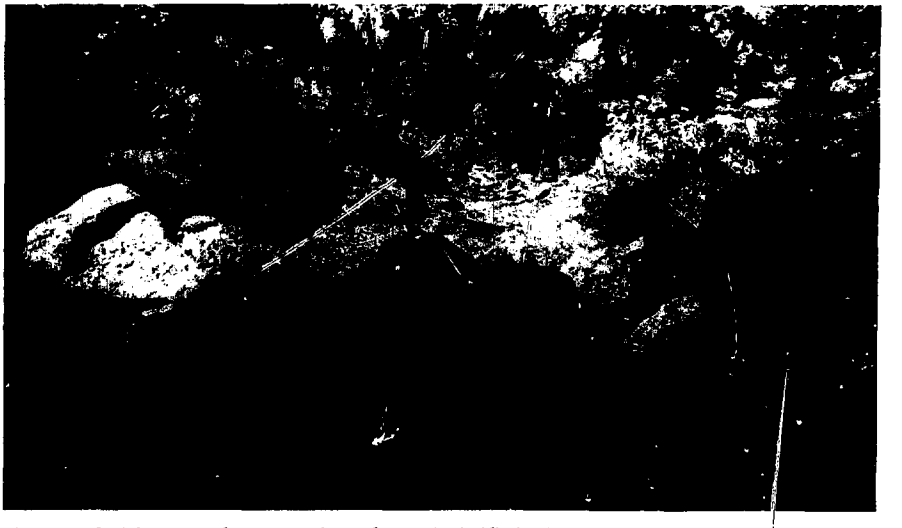

Figure 3. Thick zone of moderately welded, devitrified, slightly vapor-phase altered Bullfrog Member overlying the vitrophyre. The unit dips to the southeast (right) and is well jointed. Samples were collected from this zone for the Waste Package experimental work.

Figure 4. The Bullfrog Member is overlain by a breccia consisting of Bullfrog related material, indicating the relative proximity to the Bullfrog caldera since the breccia owes its existence to caldera collapse. Note the large size of material incorporated in the breccia.

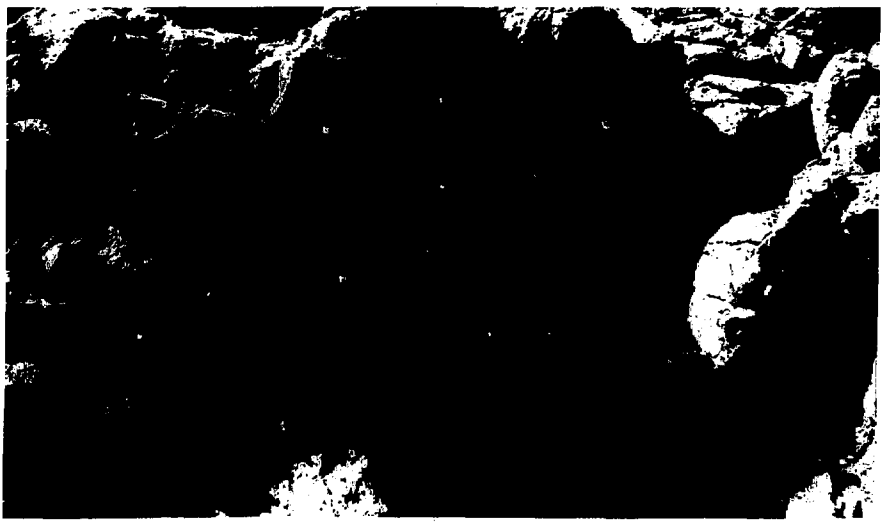

Figure 5. Close-up view of material sampled for Waste Package experimental work. Note the fractured nature of the tuff and the well-developed joint sets.

and fractures. These trimmed blocks were then either cored or slabbed in preparation for crushing. A thin section from a sample of the slabbed material was used for this characterization. The slabbed material was then crushed to mm size with a jaw crusher with alumina plates and then pulverized with a Spex mill with a tungsten carbide vessel and ball for Batch A or alumina plates for Tcfb and Batch B. The Batch A and B material used for NAA characterization was sieved to 140 mesh. The XRD sample was prepared by further pulverizing the Tcfb samples (−140 mesh) to −325 mesh with a Spex mill. Analytical conditions used during each characterization procedure are described in the appropriate section.

Petrographic Description

Detailed descriptions of the petrography of the Tcfb have been provided by several reports cited in the Introduction. A point count was not made using the thin section prepared here; rather, the general characteristics and approximate modes were noted for comparison with these previous descriptions.

Observations in transmitted light with a Leitz Orthoplan petrographic microscope show the rock to be a partially to moderately welded, devitrified, partially vapor-phase altered ash flow tuff. The vitric components display a variety of textural features. Some shards are quite distinct, yellow-brown to red brown in color against a light tan to dark brown groundmass. The shards, which are frequently aligned and draped around phenocrysts, usually have an axiolitic texture and are completely replaced by very fine grained devitrification products. No glass was observed. Pumice ranged from nearly undeformed to flattened. Some pumice fragments contain spherulites near borders and throughout their centers. Many pumice have red-brown border regions that later EMP analyses will show to be iron rich. Some pumice display a nearly granophyric texture of tightly packed devitrification products. The vitric textures would suggest both primary devitrification and vapor phase alteration followed to some degree by a diagenetic recrystallization. Figures 6–8 show

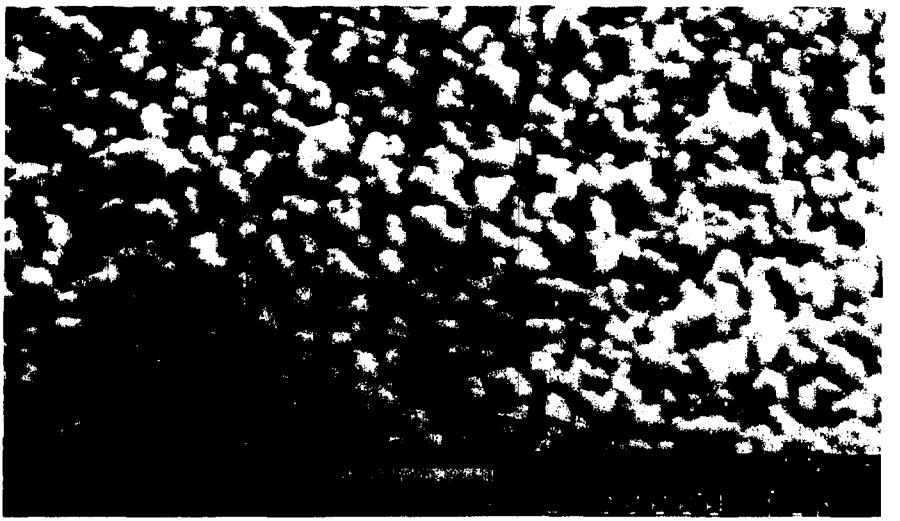

Figure 6. Backscattered electron image of a fractured surface of Bullfrog Member tuff. This material can vary compositionally from quartz to alkali feldspar on a submicron scale.

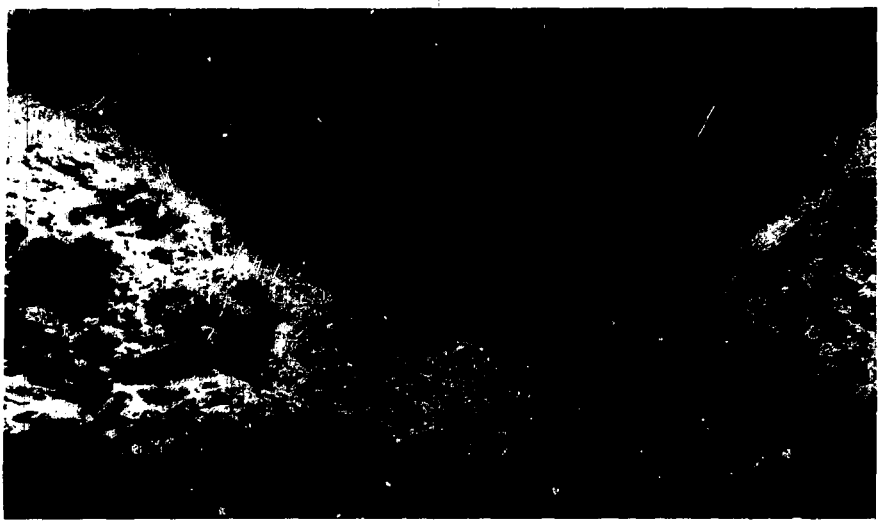

Figure 7. Backscattered electron image of vapor-phase deposited material, primarily alkali feldspar, within a vug.

Figure 8. Backscattered electron image of fine-grained quartz and alkali feldspar within a vug.

the extremely fine-grained nature of these devitrification and vapor-phase products. Both fine granular and fibrous devitrification products consisting of intergrown silica and K-feldspar are shown.

The vitric components comprise about 85–90% of the rock. The phenocrysts making up the remainder of the rock consist of subequal amounts of sanidine and plagioclase, less quartz, minor biotite, minor magnetite, rare ilmenite and hornblende, and trace zircon and apatite, and no zeolites. Some comments regarding the appearance of the phenocrysts are warranted. The quartz are large and wormy-resorbed and embayed (Fig. 9). The sanidine and plagioclase are also large but are not resorbed, for the most part. The biotite (Fig. 10) and hornblende (Fig. 11) are relatively fresh looking, although the edges of biotite are sometimes blackened. This differs from most descriptions of these mafic phases in Tcfb beneath Yucca Mountain, with the exception of G-1. These observations (and field evidence based on an absence of zeolites in the nonwelded materials in this section) suggest that at this locality the Tcfb has never been below the static water level.

The rock is relatively porous and contains fractures either open or filled with silica or hematite. As will be shown in a subsequent report (Knauss, 1983), the specific surface area of core wafers used in hydrothermal experiments is nearly as high as that of crushed tuff, attesting to the high interconnected porosity.

Based strictly on a cursory petrographic analysis, the interval sampled at the Tcfb outcrop appears to correspond to about the 2400 ft level in G-1. Although no cooling break was observed at this locality in the Tcfb section, the presence of a developed vitrophyre suggests we are in a position equivalent to the most densely welded material within the so-called BF-II unit (Bish et al., 1981). The abundance and size of phenocrysts and the vitric component textures observed here match most descriptions between about 2320 and 2420 ft relative to G-1.

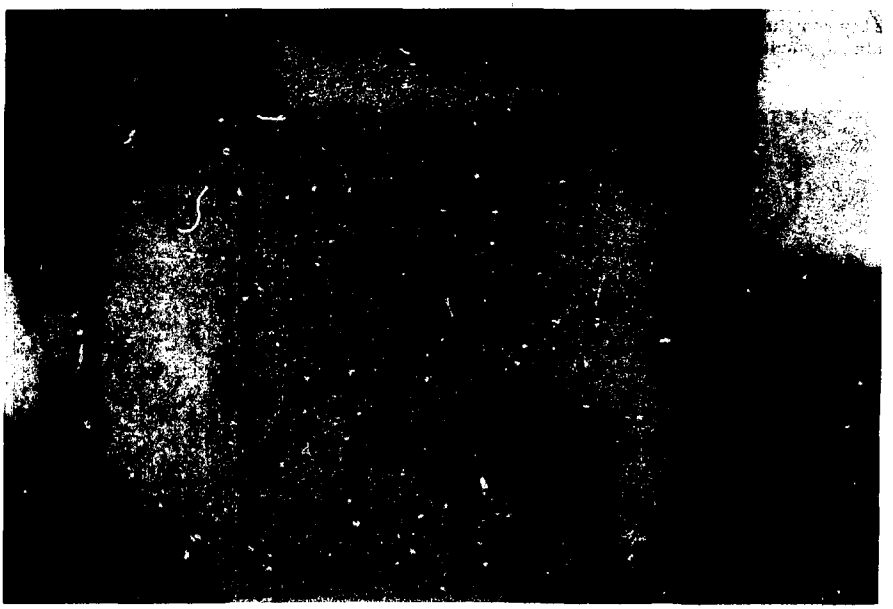

Figure 9. Large wormy-resorbed and embayed quartz phenocrysts are common within the Bullfrog Member. The photomicrograph is spanning approximately 1.5 mm in the longest dimension.

Figure 10. The biotite phenocryst in this Bullfrog Member section is fairly fresh looking in the central zone from which samples were collected. The edges may be somewhat blackened, however. They contain numerous included phases such as zircon and apatite. The photomicrograph is spanning approximately 1.5 mm in the longest dimension.

Figure 11. The hornblende phenocryst is a much less common mafic than biotite and is a relatively fresh variety. The photomicrograph is spanning approximately 1.5 mm in the longest dimension.

Bulk Mineralogy via XRD

In order to characterize the bulk mineralogy of Tcfb, three samples of material (Batch A, Batch B, and a separate hand sample) were analyzed by XRD. The sample powders were run on an automated powder diffractometer from 2° to at least 40° 2θ using Cu-K_α radiation and computerized data recording. The spectra were then analyzed by computer for peak identification and calculation of d-spacing, relative intensity, and peak area. This system is presently being calibrated with standards to allow determination of phase proportions (semi-quantitative analysis). The data for these samples recorded on diskette can be so analyzed at a future date.

The XRD spectra recorded were essentially identical. Figure 12 shows the Batch B spectra. Table 1 lists the derived peaks. Phases present in amounts easily detectable include alkali feldspar, quartz, α-cristobalite, muscovite/illite, and amphibole. Notably absent are peaks for tridymite or any of the zeolites encountered at Yucca Mountain. The broad glass peak centered about a d-spacing of 4 Å is also absent. Although not identified as a distinct peak, there is a bulge on the shoulder of the x-ray beam peak at low angle above the background inferred by drawing a smooth curve. This bulge occurs in the general vicinity of montmorillonite and may correspond to the tan to red-brown material, which rims the pumice fragments and is disseminated throughout the matrix. An effort was made to confirm or deny the presence of clays using SEM. Vugs exposed by cutting core wafers were examined, and, as Fig. 13 shows, some clay-like phases were present. These phases were very rare, however, and most clay in the Tcfb is disseminated throughout the matrix (rimming pumice fragments and shards) or lining fractures.

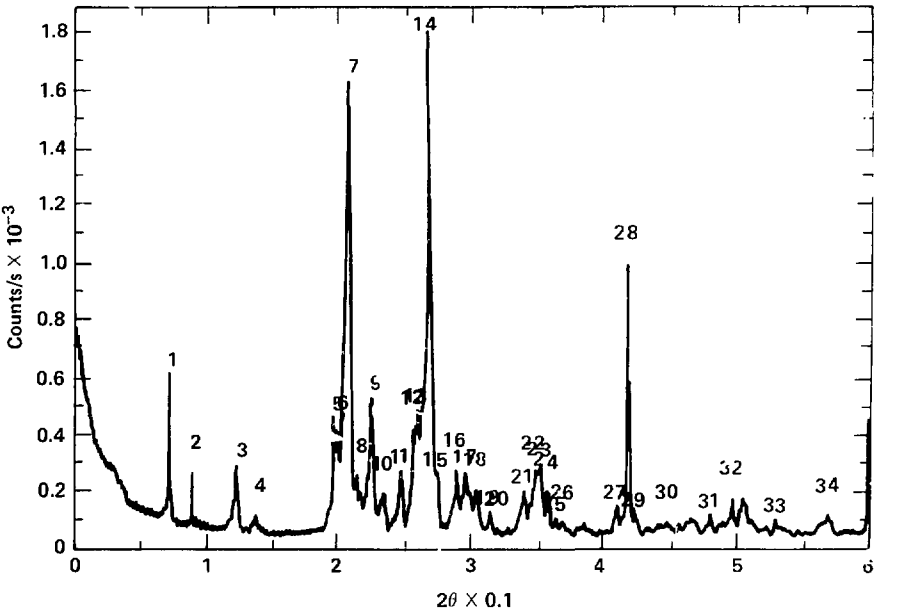

Figure 12. X-ray diffraction spectra of Bullfrog Member used in Waste Package experimental work. The spectra were collected using an automated powder diffractometer and computerized data reduction system. Semi-quantitative analysis of phase proportions may be made using this system. The presence of minor smectite is indicated by the bulge in the smoothly decreasing curve of scattered x rays from the beam.

Table 1. X-ray diffraction peaks identified by computer in the Bullfrog Member tuff used in Waste Package experimental work. Phases present include alkali feldspar, quartz, alpha cristobalite, muscovite/illite, and amphibole. Notably absent are peaks for tridymite, zeolite, and glass.

Peak #	D-space	Height	Area	Width
1	9.9938	33.8	21.9	0.242
2	8.4342	15.1	7.5	0.187
3	6.4292	16.3	12.3	0.283
4	5.8390	6.7	6.1	0.342
5	4.2595	25.7	19.4	0.284
6	4.2028	23.2	11.5	0.186
7	4.0511	90.0	100.0	0.216
8	3.9310	14.5	9.7	0.250
9	3.7664	29.3	32.5	0.415
10	3.6096	10.8	9.7	0.338
11	3.4499	15.1	13.3	0.332
12	3.3335	23.8	15.4	0.242
13	3.2994	27.4	18.7	0.256
14	3.2155	100.0	78.4	0.294
15	3.1398	15.2	11.0	0.270
16	2.9877	15.4	16.5	0.401
17	2.9228	15.0	13.7	0.342
18	2.8500	11.5	8.2	0.267
19	2.7642	7.2	6.2	0.319
20	2.7152	4.0	3.7	0.351
21	2.5729	11.2	7.5	0.251
22	2.5198	15.0	13.3	0.331
23	2.4953	16.7	12.0	0.270
24	2.4585	11.5	8.4	0.273
25	2.4149	6.3	5.7	0.343
26	2.3803	5.5	7.7	0.523
27	2.1671	8.1	8.6	0.398
28	2.1303	54.9	31.1	0.212
29	2.1035	7.8	5.1	0.246
30	1.9976	5.3	6.3	0.442
31	1.8761	6.7	6.0	0.338
32	1.8185	10.0	10.5	0.394
33	1.7191	5.7	5.0	0.325
34	1.6101	6.4	5.8	0.339

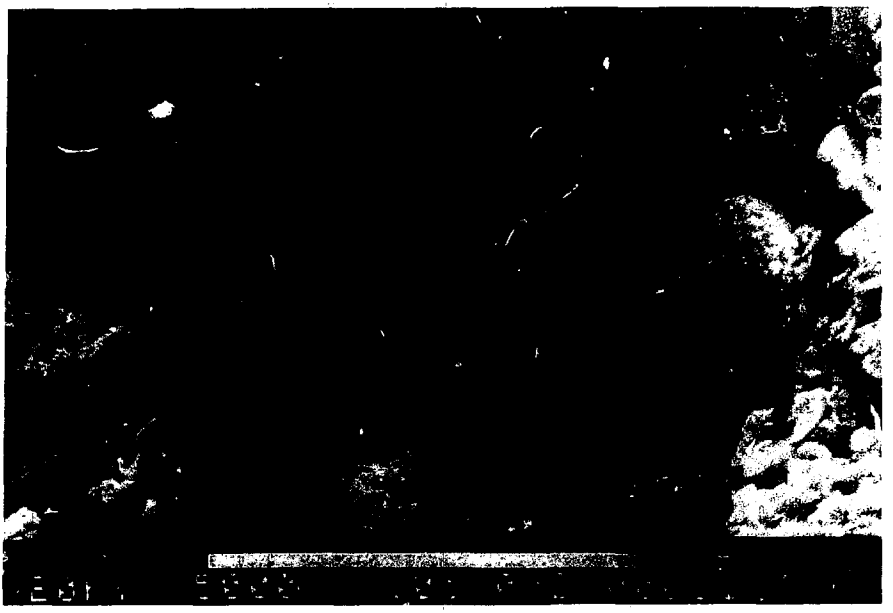

Figure 13. Backscattered electron image of clay-like phase within a vug.

Bulk Chemistry via NAA

Samples from both Batch A and B were analyzed by NAA for a suite of elements. Approximately 200 mg of −140-mesh material was mixed with an equal amount of Avicel binder and pelletized. The samples were irradiated for 72 min at a flux of 1.9×10^{13} n/cm^2·sec. After cooling times of 4 d, 21 d, and 40 d, the samples were counted for periods of 8000 s, 20,000 s, and 20,000 s, respectively, with an automated Ge (Li) gamma spectrometer. Nuclide identification and quantification were done by the GAMANAL code, activity data were converted to composition by NADAC, and the results of multiple count data for each element were combined by the MERGE code. Although not used in calculating sample concentrations (because GAMANAL works with absolute activity), each irradiation and count contains an appropriate USGS standard rock as a check standard.

Table 2 summarizes the data obtained for the two Tcfb samples analyzed. As can be readily seen, Batch A material has been contaminated by the tungsten carbide vessels. It contains anomalous values for Cr, Co, Ni, and W. Fortunately, only a few of the first rock/water interaction experiments were done with Batch A material. These were repeated at a later date with Batch B material. Batch A remained useful for all thermomechanical experiments. The data for the two analyses agree reasonably well and give some feeling for the approximate sample variability one might expect to encounter in closely spaced samples.

Table 2. Results for neutron activation analysis of two samples of Bullfrog Member tuff. The Batch A material was prepared in a tungsten carbide Spex mill and found to contain traces of Cr, Co, Ni, and W not present in the tuff. Batch B is the material used in all rock/water interaction studies with the exception of the very first (preliminary) experiment.

Element (ppm)	Tcfb-A[a]	Tcfb-B[b]
Na (10^4)	3.453 ± 0.059	3.025 ± 0.078
K (10^4)	4.859 ± 0.379	3.799 ± 0.274
Ca (10^4)	nd[c]	nd[c]
Fe (10^4)	1.015 ± 0.017	1.097 ± 0.012
Sc	1.226 ± 0.012	1.294 ± 0.016
Cr	60.54 ± 0.81	nd[c]
Co	2.887 ± 0.167	0.537 ± 0.033
Ni	34.90 ± 4.68	nd[c]
Zn	38.36 ± 8.69	73.78 ± 3.37
As	5.883 ± 0.906	7.578 ± 1.197
Rb	97.84 ± 4.93	150.5 ± 2.2
Sr	127.8 ± 19.5	259.9 ± 23.0
Zr	255.7 ± 45.3	247.4 ± 35.1
Mo	nd[c]	45.63 ± 7.68
Sb	0.404 ± 0.055	0.484 ± 0.047
Cs	3.007 ± 0.115	2.903 ± 0.078
Ba	330.9 ± 43.5	669.2 ± 16.89
La	80.31 ± 1.28	70.71 ± 0.62
Ce	105.3 ± 0.9	142.5 ± 1.84
Nd	45.28 ± 19.41	45.25 ± 4.32
Sm	7.289 ± 0.267	7.695 ± 0.194
Eu	0.293 ± 0.042	0.739 ± 0.019
Gd	91.82 ± 25.34	8.223 ± 2.952
Tb	0.576 ± 0.065	0.826 ± 0.019
Yb	3.271 ± 0.146	3.743 ± 0.083
Lu	0.570 ± 0.030	0.601 ± 0.020
Hf	5.012 ± 0.139	7.361 ± 0.113
Ta	1.972 ± 0.088	1.561 ± 0.034
W	75.05 ± 3.80	nd[c]
Au	0.0071 ± 0.0066	nd[c]
Th	15.94 ± 0.31	20.98 ± 0.19
U	2.495 ± 0.353	4.438 ± 0.257

[a] Pulverized in a tungsten carbide Spex Mill.

[b] Pulverized in a high-purity alumina, flat-plate grinder.

[c] Not detectable.

Surface Area of Crushed Tuff

The surface area of batches of crushed Tcfb used in Waste Package experiments was determined. Both Ar and N_2 BET gas adsorption methods were used. The results are shown below:

Tcfb-A	#1	5.07	m^2/g	(Ar)
Tcfb-A	#2	5.06	m^2/g	(Ar)
Tcfb-A	#3	6.25	m^2/g	(N_2)
Tcfb-B	#1	3.83	m^2/g	(Ar)
Tcfb-B	#2	3.79	m^2/g	(Ar)
Tcfb-B	#3	4.79	m^2/g	(N_2)

The results are quite consistent with N_2 surface areas about 20% higher than Ar, which is usually the case. The two batches prepared do have distinctly different specific surface areas with Batch B about 25% lower than Batch A.

Analytical Mineralogy

There are several reasons why it is necessary to know both the whole rock geochemistry and the mineralogy and individual phase chemistry of rock used in waste package experiments. Warren and co-workers at LANL (Bish et al., 1981) have shown the potential for using phenocryst geochemistry to define/distinguish/correlate tuff formations or members and to recognize relative position within eruptive units. The waste package aqueous environment after waste emplacement will be determined by complex interactions involving dissolution/precipitation kinetics and thermodynamic equilibrium. These interactions are a function of the individual phase chemistry of the tuff rather than the whole rock geochemistry. Finally, to fully understand the sources and sinks for dissolved species (mass balance), one must consider more than just the evolution of the aqueous phase in hydrothermal rock/water interaction experiments.

To geochemically characterize the individual phases in Tcfb, both the polished thin section and a polished core wafer were examined by SEM and analyzed by qualitative EDS and quantitative WDS with an automated electron microprobe (EMP). The JEOL 733 Superprobe was typically operated (for EDS and WDS) at a 15-kV accelerating potential, a 15-nA (or less) beam current, and a 100-μ^2 rastered beam. Smaller beam areas were used with correspondingly lower beam current where required. To minimize volatile loss, Na and K were always counted first in the automated schedule of analyses. Elements were calibrated against appropriate well-characterized silicate standards provided by Charles Taylor, Co., Palo Alto, CA. Oxide weight percentages reported in Table 3 were calculated with a Bence-Albee correction scheme.

The results of quantitative EMP analyses are listed in Table 3 and grouped by phase. Note that pumice or matrix data are analyses of a mixture of phases, i.e., quartz and alkali feldspar, on a micron to submicron scale. Phenocrysts were analyzed at their cores, unless otherwise noted.

As shown by Warren (Bish et al., 1981), the dominant value and range of the most important compositional components are frequently invariant for a single ash-flow sequence and can be recognized in histograms. They are thus correlative tools for these units. Alternatively, similarities among mineral compositions between units may define petrographic suites. Histograms were made to show variation in potassium (orthoclase molecular end member, Fig. 14) in alkali feldspar, calcium variation (anorthite molecular end member, Fig. 15) in plagioclase, and magnesium/iron variation (Mg/Mg + Fe) in both biotite (Fig. 16) and amphibole (Fig. 17). Note that more samples are plotted than tabulated in this report, because only thin-section data were tabulated here. The tabulated data for the reference Tcfb core wafer are presented in another report (Knauss, 1983). The histogram, however, contains data from both sources, although individual histograms of thin-section vs core wafer are indistinguishable and are combined simply to improve statistics. Although quartz, magnetite, ilmenite, zircon, and apatite were also observed in thin-section, no analyses are presented here. A few analyses for these phases are included in the Tcfb core wafer report mentioned above.

Table 3. Results of quantitative electron microprobe analyses using wavelength dispersive methods and Bence-Albee data reduction schemes. Analytical conditions used on the fully automated system are detailed in the text.

Table 3a. Biotite.

Oxide	1.1	1.2	1.3	1.4	2.1	2.2	2.3	2.4	4.1	4.2	4.3	4.4[a]
SiO_2	36.30	35.43	35.56	35.55	37.38	37.24	37.43	37.79	36.24	35.22	36.92	37.09
Al_2O_3	13.96	14.31	13.25	14.39	16.08	15.49	15.63	15.80	13.97	13.92	14.44	13.48
K_2O	8.76	8.72	8.87	9.14	8.40	8.30	8.55	8.54	8.55	8.73	8.71	9.07
Na_2O	0.56	0.54	0.51	0.52	0.78	0.83	0.79	0.79	0.57	1.55	0.52	0.55
CaO	0.00	0.03	0.04	0.00	0.02	0.02	0.03	0.04	0.02	0.00	0.05	0.02
FeO	26.14	24.93	24.81	24.38	14.89	15.01	14.88	15.10	24.92	24.48	24.15	24.37
MgO	10.61	8.78	8.55	9.60	14.85	15.01	14.59	14.35	9.16	9.24	8.98	9.04
MnO	–	–	0.31	0.81	–	–	–	0.40	–	–	–	0.84
TiO_2	4.40	4.43	4.36	4.33	4.52	4.42	4.50	4.66	3.85	4.52	4.62	4.54
F	–	–	0.05	0.00	–	–	–	0.00	–	–	–	0.12
Cl	–	–	2.22	1.85	–	–	–	0.72	–	–	–	1.82
Total	101.41	98.29	98.52	100.59	98.19	97.70	97.41	98.19	97.53	98.04	98.57	100.93
Ti/Fe	0.152	0.160	0.158	0.160	0.273	0.265	0.272	0.278	0.139	0.166	0.172	0.168
Mg/Mg + Fe	0.422	0.388	0.383	0.415	0.642	0.643	0.638	0.631	0.398	0.405	0.401	0.400

Oxide	9.1	9.2	9.3	10.1	10.2	10.3	10.4	12.1	12.2	12.3	12.4[a]
SiO_2	36.65	36.77	36.08	35.85	36.07	36.75	37.02	35.62	34.42	35.75	33.37
Al_2O_3	14.36	13.56	13.43	14.05	14.38	13.29	13.54	14.47	14.74	13.82	16.94
K_2O	8.63	8.44	8.74	8.59	8.62	8.60	8.70	8.52	8.38	8.02	8.50
Na_2O	0.53	0.48	0.54	0.60	0.56	0.50	0.55	0.49	0.54	0.54	0.45
CaO	0.01	0.00	0.00	0.00	0.00	0.00	0.07	0.00	0.00	0.00	0.11
FeO	25.37	24.18	24.68	25.10	25.16	24.27	24.73	25.47	25.39	25.22	24.72
MgO	8.55	8.75	8.48	8.59	8.69	8.52	8.57	7.78	8.42	9.05	7.91
MnO	–	–	0.78	–	–	–	0.80	–	–	–	0.79
TiO_2	4.32	4.91	4.95	4.40	4.27	4.63	4.82	4.14	4.71	4.64	4.[illegible]
F	–	–	0.00	–	–	–	0.00	–	–	–	0.00
Cl	–	–	1.66	–	–	–	1.54	–	–	–	1.86
Total	99.40	97.99	97.36	98.68	99.29	97.60	100.33	98.07	98.08	98.39	99.51
Ti/Fe	0.153	0.183	0.181	0.158	0.153	0.172	0.175	0.146	0.167	0.166	0.177
Mg/Mg + Fe	0.377	0.394	0.382	0.381	0.383	0.387	0.384	0.355	0.374	0.392	0.366

Oxide	15.1	15.2	15.3	18.1	18.2	18.3	20.1	20.2[a]
SiO_2	35.70	35.64	34.43	37.22	35.87	36.77	36.34	36.67
Al_2O_3	13.90	13.74	14.05	14.25	14.32	13.38	13.03	13.17
K_2O	8.37	7.99	8.72	9.07	8.84	8.95	8.73	8.83
Na_2O	0.54	0.66	0.53	0.61	1.40	0.55	0.52	1.28
CaO	0.09	0.08	0.04	0.00	0.02	0.03	0.00	0.03
FeO	24.35	24.80	24.75	23.55	23.26	22.79	24.27	22.96
MgO	8.39	8.66	8.36	9.98	9.78	9.96	10.03	8.99
MnO	–	–	0.80	–	–	0.73	–	–
TiO_2	4.62	4.50	4.63	4.04	4.51	4.60	4.20	4.15
F	–	–	0.00	–	–	1.48	–	–
[illegible]	–	–	1.76	–	–	1.68	–	–
[illegible]	97.21	96.72	98.07	98.74	98.00	100.94	97.14	96.07
[illegible]	0.171	0.163	0.168	0.154	0.175	0.182	0.156	0.163
[illegible]	0.383	0.369	0.378	0.433	0.431	0.440	0.427	0.413

[illegible] photo number and y = point number.

Table 3b. Hornblende.

Oxide	5.1	8.1	13.1	13.2	13.3	19.1	19.2[a]
SiO_2	42.78	43.13	45.61	45.73	46.72	43.70	44.34
Al_2O_3	12.16	9.43	7.01	6.94	6.59	7.59	7.48
K_2O	0.60	0.81	0.70	0.53	0.58	0.75	0.69
Na_2O	2.12	1.93	1.81	1.76	1.79	1.82	1.77
CaO	11.05	10.49	9.74	10.07	10.04	9.65	9.30
FeO	12.35	20.92	22.09	21.50	21.00	21.68	20.76
TiO_2	2.17	1.69	1.17	1.28	1.41	1.41	1.46
MgO	13.25	8.73	9.51	9.20	9.02	8.63	8.52
MnO	0.32	1.48	1.35	1.75	1.65	1.72	1.52
F	0.00	0.00	0.00	0.07	0.00	0.00	0.05
Cl	0.00	0.00	0.00	0.00	0.00	0.00	0.00
Total	96.80	98.62	98.99	98.85	98.83	96.94	95.90
Ti/Fe	0.158	0.073	0.048	0.054	0.061	0.058	0.063
Mg/Mg + Fe	0.659	0.429	0.437	0.435	0.436	0.417	0.425

Table 3c. Matrix.

Oxide	4.1	4.2	10.1	16.1	16.2	18.1[a]
SiO_2	76.41	80.15	77.37	85.65	70.94	74.75
Al_2O_3	15.14	12.70	12.06	6.50	15.71	13.32
K_2O	4.31	1.16	4.42	3.66	8.79	7.17
Na_2O	3.91	3.68	3.10	1.07	2.62	2.76
CaO	0.80	1.03	0.39	0.10	0.29	0.31
MgO	0.05	0.02	0.03	0.06	0.06	0.00
FeO	0.19	0.38	0.60	0.94	0.94	0.25
TiO_2	0.22	0.06	0.04	0.00	0.19	0.25
MnO	0.00	–	0.04	–	0.08	0.00
BaO	0.00	0.00	0.00	0.19	0.00	0.00
Total	101.19	99.19	98.16	98.17	99.68	98.87
Qz	33.75	–	40.52	–	20.06	29.22
Or	26.17	–	27.82	–	54.19	43.64
Ab	36.03	–	29.61	–	24.50	25.49
An	4.05	–	2.06	–	1.25	1.34

Table 3d. Plagioclase.

Oxide	8.1	8.2	14.1	14.2	14.3	15.1	17.1	20.1[a]
SiO_2	65.05	62.85	64.16	65.21	65.26	61.75	63.33	63.64
Al_2O_3	23.12	23.12	24.86	24.30	23.22	26.02	23.35	23.49
K_2O	1.16	1.31	0.99	1.15	1.33	0.62	1.17	1.26
Na_2O	8.64	8.67	7.91	8.34	7.87	7.30	8.59	8.58
CaO	2.99	3.07	4.13	3.55	3.13	5.99	3.33	3.17
MgO	0.00	0.00	0.00	0.00	0.00	0.00	0.03	0.05
TiO_2	0.00	0.00	0.10	0.00	0.00	0.00	0.08	0.05
FeO	0.00	0.14	0.00	0.00	0.13	0.25	0.17	0.11
BaO	0.00	0.09	0.00	0.00	0.00	0.08	0.30	0.00
Total	100.96	99.25	102.15	102.55	100.95	102.01	100.35	102.34
Qz	–	–	–	–	–	–	–	–
Or	6.94	7.71	5.99	6.87	8.38	3.70	6.87	7.42
Ab	78.09	77.16	72.93	75.39	75.08	66.21	76.68	76.86
An	14.98	15.13	21.08	17.34	16.54	30.08	16.46	15.72

Table 3e. Sanidine.

Oxide	1.1	9.1	10.1	19.1[a]
SiO_2	67.24	66.74	67.27	64.23
Al_2O_3	19.92	20.14	20.08	22.51
K_2O	10.67	10.72	10.71	10.41
Na_2O	3.93	3.96	4.00	3.80
CaO	0.23	0.23	0.21	0.23
MgO	0.01	0.00	0.06	0.01
TiO_2	0.00	0.00	0.12	0.00
FeO	0.18	0.18	0.16	0.16
BaO	0.71	0.14	0.14	0.78
Total	102.90	102.12	102.75	102.14
Qz	–	–	–	–
Or	63.41	63.36	63.21	63.64
Ab	35.42	35.49	35.77	35.17
An	1.17	1.16	1.02	1.20

[a] x y, where x = photo number and y = point number.

Table 3f. Pumice.

Oxide	7.1	11.1	17.1[a]
SiO_2	76.29	75.43	69.20
Al_2O_3	12.83	16.14	13.51
K_2O	6.52	1.22	4.75
Na_2O	2.49	7.80	3.26
CaO	0.36	0.37	0.85
MgO	0.03	0.00	0.02
FeO	0.14	0.00	5.91
TiO_2	0.02	0.03	0.36
MnO	0.07	–	–
BaO	0.00	0.00	0.13
Total	98.73	101.00	98.78
Qz	34.69	–	–
Or	40.22	–	–
Ab	23.25	–	–
An	1.84	–	–

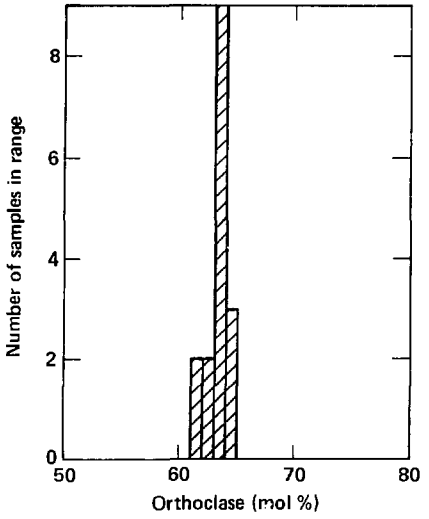

Figure 14a. Ordinary histogram of cation normative orthoclase calculated for analyzed alkali feldspar phenocrysts. The average value is about 0.63 OR.

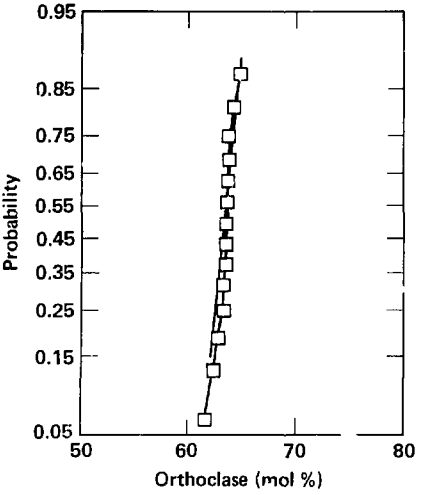

Figure 14b. Cumulative frequency plot of data presented in Fig. 14a showing presence of only one population.

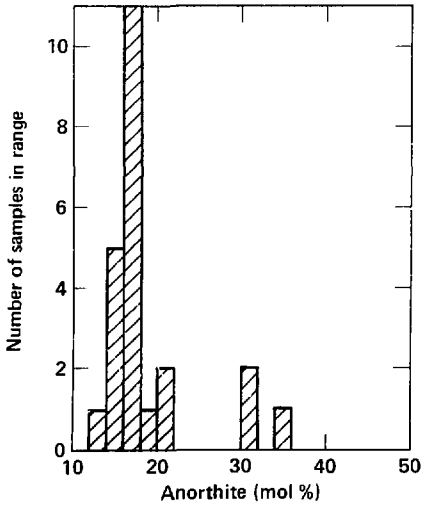

Figure 15a. Ordinary histogram of cation normative anorthite calculated for analyzed plagioclase feldspar phenocrysts. The most common value is 0.17 AN.

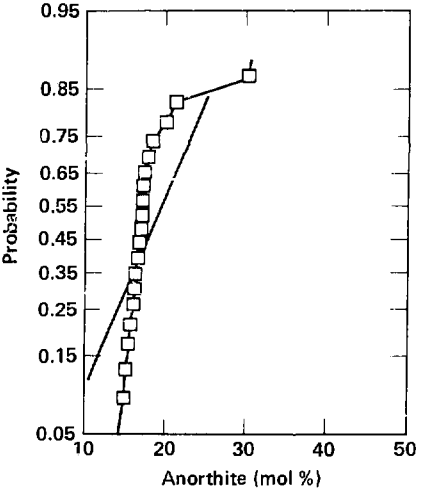

Figure 15b. Cumulative frequency plot of data presented in Fig. 15a showing a distinctly bimodal distribution.

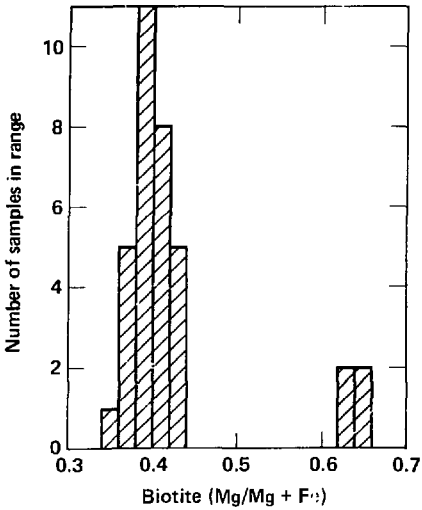

Figure 16a. Ordinary histogram of cation ratio calculated for analyzed biotite phenocrysts. The most common value for this ratio is about 0.4.

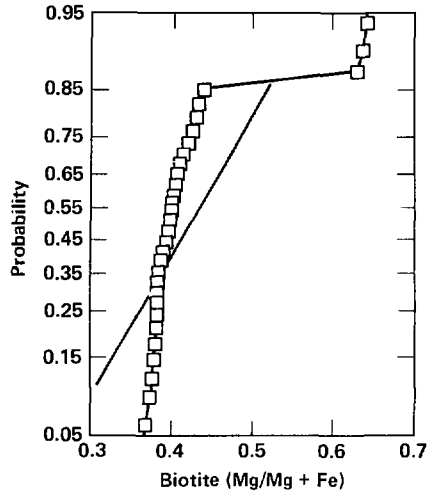

Figure 16b. Cumulative frequency plot of data presented in Fig. 16a showing a distinctly bimodal distribution with one group at 0.4 and a second at 0.6.

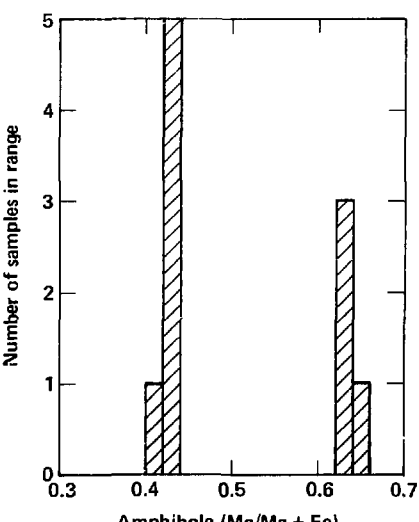

Figure 17a. Ordinary histogram of cation ratio calculated for analyzed hornblende phenocrysts. The most common value is also about 0.4.

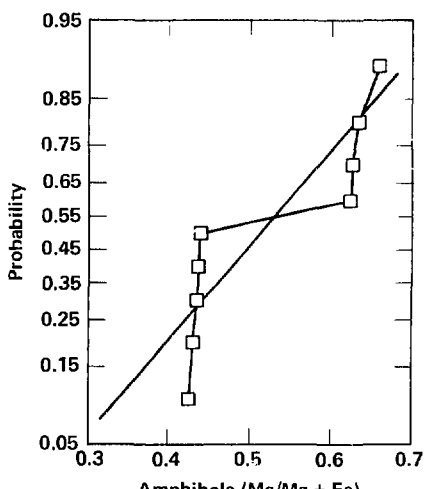

Figure 17b. Cumulative frequency plot of data from Fig. 17a showing a distinctly bimodal distribution with one group at 0.4 and another at 0.6.

The average orthoclase end member content for the alkali feldspar is 63 mol % and the distribution is normal. The range in observed values is very small, varying from 61-65 mol %. The dominant anorthite end member content of the plagioclase is 17 mol % with an average of 18.6 mol %, while the distribution is bimodal. Some of the normally zoned plagioclase cores were distinctly Ca rich, ranging up to 36 mol %. The lower limit of observed anorthite end member composition was about 12 mol %. The mafic phenocrysts, biotite and hornblende, were relatively Mg poor. For both mafics the dominant Mg/(Mg + Fe) ratio was 0.4, although the distribution was distinctly bimodal with a second group at 0.64.

The histograms for feldspar end members presented here for Tcfb outcrop samples are virtually identical to those presented by Warren (Bish et al., 1981) for hole G-1. The mafic Mg/(Mg + Fe) ratio differs, however, in that the 0.4 population observed by Warren at Yucca Mountain in G-1 is accompanied by a distinct group at 0.6. This high Mg hornblende was also observed by Warren (unpublished data, 1982) in samples from the same Lathrop Wells Tcfb section in specimens collected from the vitrophyre. Single mafic phenocrysts produce analyses clearly in only one of the two groups. The Mg-rich mafics are significantly less common than the Fe-rich mafics and are not contained within lithic fragments. Although not plotted here, the EMP data in Table 3 show the average biotite BaO weight percent to be about 0.6%, with a dominant value somewhat lower. Warren observed that in the Tcfb, the upper portion of the unit tended to have a higher BaO content (1.3%) compared to the lower portion (0.3%).

Summary

The purpose of this characterization of Tcfb is twofold: first, to provide data about the mineralogy and chemistry of the rock used in experiments supporting waste package design (geochemical modeling and corrosion, radiation damage, thermomechanical studies, etc.) and second, to verify that the outcrop material used to provide large quantities of rock for the experimental program matched reasonably well with the rock at depth beneath Yucca Mountain within the proposed Tcfb repository interval.

The basic data provided here include the following:

- Simple petrographic description.
- Relative distribution of the dominant phases.
- XRD analyses and phase identification.
- SEM phase identification.
- Nature and distribution of fractures and fillings.
- BET surface area analyses.
- NAA chemical analyses of whole rock.
- EMP quantitative chemical analyses of phases.

Field relationships suggest that the outcrop material is stratigraphically equivalent to the densely welded, devitrified, vapor-phase altered core of the BF-II subunit within the Tcfb. The material contains no zeolites and appears to be glass-free. It does, however, contain trace amounts of evaporite minerals (carbonates, borates, sulfates, nitrates, etc.) due to precipitation from meteoric waters (Oversby and Knauss, 1983). The mineralogy and nature of devitrification and vapor phase alteration products would also suggest that the material most closely matches the BF-II subunit above the 2400-ft depth (relative to G-1) and within the Tcfb interval considered suitable host rock for a repository. The BaO content of the biotites suggests the samples are from the lower rather than the upper portions of the Bullfrog Member Tuff. These outcrop samples should be acceptable representatives of the Tcfb unit beneath Yucca Mountain for experiments performed in support of Waste Package design.

The Bullfrog Member of the Crater Flat tuff is one of four Yucca Mountain tuff units that were under consideration by the Nevada Nuclear Waste Storage Investigations (NNWSI) Project as a potential location for a mined geologic repository for high-level nuclear waste. Two of the units, the Topopah Spring Member of the Paintbrush tuff and the tuffaceous beds of the Calico Hills, are located above the water table in the unsaturated zone. The other units, the Bullfrog and Tram, are located below the water table. The NNWSI Project chose the Topopah Spring Member of the Paintbrush tuff as the reference repository horizon in mid-1982. Data generated using Tcfb rock/water interaction studies are still quite useful, indeed required, for establishing the ability of the EQ3/6 geochemical modeling code to match (predict after-the-fact) experimental results. Some degree of confidence can then be placed on the use of the code for predicting conditions over the long-term for geologic units with similar mineralogy and geochemistry.

Acknowledgments

Many thanks to the following individuals, and others not specifically mentioned, for their invaluable contributions to this project. Bill Beiriger ran the XRD scans and prepared the polished thin sections and core wafers. Jan Brown did NAA sample preparation, and Bob Heft performed the irradiation, gamma analyses, and data reduction. Chuck Slettevold made the BET analyses. Bruce Crowe spent a day in the field with me and introduced me to the Tcfb section at Lathrop Wells. Rich Warren provided unpublished microprobe analyses of related samples from this section and suggested other locations for material. Rick Ryerson helped me over many pitfalls encountered during EMP analyses. He provided direct assistance and moral support, gratis. Thanks to Barbara Bryan for expert typing.

References

Bish, D. L., F. A. Caporuscio, J. F. Copp, B. M. Crowe, J. D. Purson, J. R. Smyth, and R. G. Warren (1981), *Preliminary Stratigraphic and Petrologic Characterization of Core Samples from USW-G1, Yucca Mountain, Nevada*, Los Alamos National Laboratory, Los Alamos, NM, LA-8840-MS.

Broxton, D., D. Vaniman, F. Caporuscio, B. Arney, and G. Heiken (1982), *Detailed Petrographic Descriptions and Microprobe Data for Drill Holes USW-G2 and UE25b-1H, Yucca Mountain, Nevada*, Los Alamos National Laboratory, Los Alamos, NM, LA-9324-MS.

Byers, F. M., W. J. Carr, P. P. Orkild, W. D. Quinlivan, and K. A. Sargent (1976), *Volcanic Suites and Related Cauldrons of Timber Mountain-Oasis Valley Caldera Complex, Southern Nevada*, U.S. Geological Survey, Menlo Park, CA, Prof. Paper 919, 70 pp.

Caporuscio, F., D. Vaniman, D. Bish D. Broxton, B. Arney, G. Heiken, F. Byers, R. Gouley, and E. Semarge (1982), *Petrologic Studies of Drill Cores USW-G2 and UE25b-1H, Yucca Mountain, Nevada*, Los Alamos National Laboratory, Los Alamos, NM, LA-9255-MS.

Carr, W. J. (1982), *Volcano-Tectonic History of Crater Flat, Southwestern Nevada, As Suggested by New Evidence from Drill Hole USW-VH-1 and Vicinity*, U.S. Geological Survey, Menlo Park, CA, Open File Report 82-457, 23 pp.

Heiken, G. H., and M. L. Bevier (1979), *Petrology of Tuff Units from the J-13 Drill Site, Jackass Flats, Nevada*, Los Alamos National Laboratory, Los Alamos, NM, LA-7563-MS.

Knauss, K. G. (1983), *Hydrothermal Interaction Studies of Bullfrog Tuff Core Wafers in J-13 Water at 150 °C — Quantitative Analyses of Aqueous and Solid Phases*, Lawrence Livermore National Laboratory, Livermore, CA, UCRI. Report in progress.

Orkild, P. P. (1983), *Geology of the Nevada Test Site in: Proceedings of the Monterey Containment Symp.*, Los Alamos National Laboratory, Los Alamos, NM, LA-9211-C, vol. 1, pp. 323–338.

Oversby, V. M., and K. G. Knauss (1983), *Reaction of Bullfrog Tuff with J-13 Well Water at 90 °C and 150 °C*, Lawrence Livermore National Laboratory, Livermore, CA, UCRL-53442.

Scott, R., and M. Castellanos (1982), *Preliminary Report On the Geologic Character of Drill Holes USW-GU3 and USW-G3*, U.S. Geological Survey, Menlo Park, CA, Memorandum Report.

Sykes, M. L., G. H. Heiken, and J. R. Smyth (1979), *Mineralogy and Petrology of Tuff Units from the UE25a-1 Drill Site, Yucca Mountain, Nevada*, Los Alamos National Laboratory, Los Alamos, NM, LA-8139-MS.